batteries

MDPI

Article

Comparing the Cold-Cranking Performance of Lead-Acid and Lithium Iron Phosphate Batteries at Temperatures below 0 °C

Sophia Bauknecht *, Florian Wätzold, Anton Schlösser and Julia Kowal

Electrical Energy Storage Technology, Technische Universität Berlin, Einsteinufer 11, 10587 Berlin, Germany
* Correspondence: sophia.bauknecht@tu-berlin.de

Abstract: Six test cells, two lead–acid batteries (LABs), and four lithium iron phosphate (LFP) batteries have been tested regarding their capacity at various temperatures (25 °C, 0 °C, and −18 °C) and regarding their cold crank capability at low temperatures (0 °C, −10 °C, −18 °C, and −30 °C). During the capacity test, the LFP batteries have a higher voltage level at all temperatures than LABs, which results in a higher power and energy output. Moreover, LFP batteries have a lower capacity decline and a lower energy decline for decreasing temperature. Regarding the cold-cranking test definition, the LABs passed the test at 0 °C, −10 °C, and −18 °C, but not at −30 °C. The LFP batteries passed the test at 0 °C and −10 °C. At −18 °C, only two of the four LFP batteries passed, while all LFP batteries failed the test at −30 °C. For comparability between technologies, it is suggested to redefine the requirements of the standard test in terms of power or energy. With this redefinition, the LFP battery can generate comparable cold-cranking results till −18 °C.

Keywords: low temperature; negative temperature; lead–acid battery; Pb; LAB; lithium iron phosphate battery; LiFePO4; LFP; starter battery; performance; cold-cranking; capacity

check for updates

Citation: Bauknecht, S.; Wätzold, F.; Schlösser, A.; Kowal, J. Comparing the Cold-Cranking Performance of Lead-Acid and Lithium Iron Phosphate Batteries at Temperatures below 0 °C. *Batteries* **2023**, *9*, 176. https://doi.org/10.3390/batteries9030176

Academic Editor: Michael Danzer

Received: 21 February 2023
Revised: 14 March 2023
Accepted: 16 March 2023
Published: 17 March 2023

1. Introduction

Initially, start, lighting, and ignition (SLI) batteries focused on the cranking of internal combustion engines. Since the cranking requires a specific revolution, a minimum power must be provided by an SLI battery to the starter for several seconds [1]. Typical passenger car gasoline engines require up to 2 kW, and diesel engines require up to 2.6 kW for ignition [2]. Starter batteries are currently built almost exclusively based on lead–acid enhanced flooded batteries or absorbent glass mat (AGM) batteries. The typical average current during engine starts for conventional 12 V lead–acid batteries (LABs) are in a range from 290 A to 620 A, shown in Table 1 [3]. Low temperatures increase the requirement and duration of the process [2,3]. For LABs, standardized tests are defined, providing comparable data of different products and companies [4].

Table 1. Typical average currents during ignition with a 12 V LAB [3].

Engine	−28 °C	−20 °C	0 °C	20 °C	40 °C
6-cylinder Otto	380 A	350 A	290 A	290 A	290 A
8-cylinder Otto	400 A	370 A	310 A	310 A	310 A
4-cylinder Diesel	460 A	430 A	370 A	370 A	370 A
6-cylinder Diesel	620 A	590 A	520 A	520 A	520 A

Prospectively, vehicles realize an exceeding amount of electrical functions consuming peak loads of up to 6 kW. Thereby, some car manufacturers already use up to two 12 V batteries, dedicating one to the ignition function and one to supply comfort to consumers [5]. From an architectural perspective, this trend leads to higher vehicle mass and package issues [6]. However, starter batteries based on lithium-ion batteries have been discussed lately [7,8]. In 2009, Porsche announced an 18 Ah lithium iron phosphate (LFP) starter battery as an add-on option for selected models reducing the weight by circa 10 kg [7]. Despite higher acquisition costs, this is already becoming an alternative for premium vehicles in the European, American, and Asian markets [8]. Lithium-ion batteries offer a high specific energy, high energy density, low self-discharge rate, and high rate of charge acceptance and maintain their charge performance throughout their lifetime [9]. Furthermore, the weight reduction of approximately 50% has been the main driver for 12 V lithium-ion adopters [9]. Especially LFP batteries are considered since these material components are considered to be safe [10,11]. LFP batteries provide a voltage plateau over an extensive SOC range enabling a constant voltage, and the voltage level of four LFP cells in series matches the voltage level of a LAB.

The electrolyte has a strong influence on low-temperature performance. The electrolyte of the LABs consists of sulfuric acid, which threatens to freeze, depending on its SoC, at low temperatures. The electrolyte of most commercially available LFP batteries consists of ethylene carbonate and dimethyl carbonate EC/DMC and conducting salt, e.g., $LiPF_6$. For LFP batteries, the electrolyte decomposition has a great influence on the low-temperature performance in terms of ionic mobility in the electrolyte solution as well as forming suitable surface films [12,13]. With decreasing temperature, the ion conductivity of the electrolyte will decrease [12,13] for both the LABs and the LFP batteries, which will increase the internal resistance of the battery.

Despite the currently ongoing applications, there is still no commonly used standard to evaluate the suitability of LFP batteries for starting, lighting, and ignition. A first test profile for thermal performance tests has been defined for a temperature range between −30 °C and 75 °C [14]. The cold-cranking capability is investigated with pulses of 6 kW for 0.5 s and 4 kW for 4 s, with 10 s pauses in between [14]. Even though lithium-ion batteries are not expected to be capable of retaining their cold-cranking capabilities at temperatures far below 0 °C [15], it was shown that they have a similar or even better performance compared to LABs with the same nominal capacity at −18 °C [9]. Within this work, LABs and LFP batteries are to be compared based on their capacity and cold-cranking performance. A special focus was given to the behavior at temperatures far below 0 °C. Therefore, a test regime for cold cranking was introduced and used for both technologies based on the existing standard for LABs, concluding with the comparison of the cold-cranking capability of LFP batteries to LABs.

2. Materials and Methods

To evaluate the differences between the LABs and the LFP technologies, six different batteries are compared regarding their capacity and energy output at low temperatures. For the LABs, one 12 V, 50 Ah 6 series (S) 1 parallel (P) and one 12 V, 92 Ah 6S1P from the same company were tested. The LFP battery packs are built based on two different 26,650 cells: two 12 V, 25 Ah 4S10P batteries; one 12 V, 40 Ah 4S15P; and one 12 V, 50 Ah 4S20P, originating from different companies, were tested. For all six different test batteries, the battery size, the nominal capacity, and the capacity measured at 25 °C are summarized in Table 2. Due to procurement reasons, starter batteries numbers 5 and 6 were charged with an external battery management system (BMS). In contrast, the other LFP batteries (numbers 3 and 4) included an internal battery management system. The operations of the internal BMS are unknown. However, for battery number 3, the BMS was bypassed during discharging tests, and for battery number 4, it was possible to reprogram the cut-off voltage during discharge to 8 V (cell cut-off voltage is 2 V) instead of the initially preprogrammed 10 V. As external BMS the KISS active from Faktor GmBH was used. This BMS contains active balancing during charging. The BMS was disconnected during the discharging tests.

Table 2. Investigated batteries.

ID	Nominal Capacity	Measured C_{20} Capacity at 25 °C	Battery Layout	Company	Internal Resistance at 25 °C	Weight	Dimensions
LAB 1	50 Ah	53.3 Ah	6S1P	A	6.55 mΩ	12.5 kg	207 × 175 × 190 mm
LAB 2	92 Ah	98.4 Ah	6S1P	A	3.05 mΩ	27.0 kg	352 × 175 × 190 mm
LFP 1	40 Ah	39.2 Ah	4S15P	B	3.33 mΩ	7.0 kg	277 × 175 × 190 mm
LFP 2	25 Ah	25.8 Ah	4S10P	C	5.35 mΩ	4.4 kg	220 × 120 × 190 mm
LFP 3	25 Ah	24.6 Ah	4S10P	D	2.94 mΩ	3.4 kg	107 × 135 × 150 mm
LFP 4	50 Ah	50.5 Ah	4S20P	D	4.17 mΩ	6.6 kg	210 × 135 × 150 mm

Before any low-temperature evaluation, all batteries were conducting two complete capacity turnovers with moderate discharging currents at 25 °C. Therefore, the starting conditions, such as the capacity, could be recorded, and further testing at low temperatures starts with freshly charged batteries. The charging of the batteries was always conducted at 25 °C. If a battery had previously completed any test at low temperatures, it was warmed up to 25 °C for 24 h before charging. The LABs were always charged according to the EN standard [4]. The EN standard defines a charge for an AGM battery with a current of $1{\cdot}I_{20} = \frac{1}{20}C$ for 24 h with a maximum voltage limit of 14.8 V [4]. The LFP batteries are charged with a charging current of 1C and a voltage limit of 14.4 V till a cut-off current of 0.05 A Ah^{-1} is reached. Thereby, the charging regime of LABs is much longer than for LFPs, ensuring the dissolution of lead sulfate crystals, enhancing lifetime, and enabling comparable results between the tests. To enable comparable results for LFP batteries, a BMS with balancing is needed during charging.

The testing procedure is schematically visualized in Table 3. Two main tests are evaluated to compare the characteristics of LABs and LFP batteries at low temperatures. The first is the C_{20} capacity test. Thereby, the discharging capacity of all batteries was tested using a low constant current of $\frac{1}{20}C$, or in LABs, in terms of I_{20}, till a cut-off voltage of 10.5 V as defined in the EN standard for lead–acid batteries [4]. The discharging currents are stated in Table 4. The low discharging currents used within this test are chosen to minimize the temperature gradient within the battery and during the test. The C_{20} test is conducted for different temperatures, such as 25 °C, 0 °C, and −18 °C, within the stated order. For temperatures other than 25 °C, the batteries are cooled down inside a climate chamber to the target temperature for 24 h before starting the capacity test. The C_{20} capacity test is conducted inside the same climate chamber, with an accuracy of ±0.25 °C.

Table 3. Test matrix.

Test Sequence	Ambient Temperature	Focus
1st Test	25 °C	
2nd Test	0 °C	C_{20} Capacity Test
3rd Test	−18 °C	
4th Test	0 °C	
5th Test	−10 °C	Cold-Cranking Test
6th Test	−18 °C	
7th Test	−30 °C	

After conducting the three capacity tests at different temperatures, the cold-cranking performance is tested at different temperatures according to the EN standard defined for lead–acid batteries [4]. The previously fully charged batteries were cooled down for 24 h to the target temperature. Within this work, tests were performed for different temperatures extending the investigation scope of the EN standard of −18 °C [4] by testing first at 0 °C, second at −10 °C, third at −18 °C and last at −30 °C.

Table 4. C_{20} capacity and cold-cranking currents.

	C_{20} Capacity Test	Cold-Cranking Test	
ID	Discharge Current	Discharge Current 1st Pulse	Discharge Current 2nd Pulse
LAB 1	2.5 A	450 A	270 A
LAB 2	4.6 A	828 A	497 A
LFP 1	2 A	360 A	216 A
LFP 2	1.25 A	255 A	135 A
LFP 3	1.25 A	225 A	135 A
LFP 4	2.5 A	450 A	270 A

The test procedure defined by the standard includes a first 10 s discharging pulse with a current of 9 A Ah^{-1} down to a cut-off voltage of 8 V, followed by a 10 s pause, finishing with a second discharging pulse with a current of 5.4 A Ah^{-1} down to a cut-off voltage of 6 V [4]. The second discharging pulse is originally not limited by time but by a cut-off voltage. However, the discharge will be stopped after 170 s if the cut-off voltage limit is not reached by that time. The discharging currents during the first and the second pulse of the cold-cranking test are stated in Table 4.

3. Results and Discussion

3.1. Capacity Test

The voltage decline over time during the constant current discharge of the capacity test is shown in Figure 1 for different temperatures. It is shown that independent of the temperature, all voltages of the LABs behave similarly. Furthermore, the voltages of all LFP batteries behave similarly as well but differently than the LABs. Figure 1a shows the C_{20} test results at 25 °C. At 25 °C, all batteries are close to meeting their target capacity. Furthermore, it must be noted that even if both technologies (LABs and LFP batteries) have comparable nominal voltages, the LFP batteries have a higher voltage level and a more stable voltage plateau during operation at all ambient temperatures. At lower temperatures, as shown in Figure 1b,c, the capacity of all batteries decreases. However, the capacity of the LABs decreases more significantly than the capacity of the LFP batteries. Furthermore, the differences between the capacity of the same technology (especially for the LABs) increase as well. Therefore, the LFP batteries have a higher power and energy output.

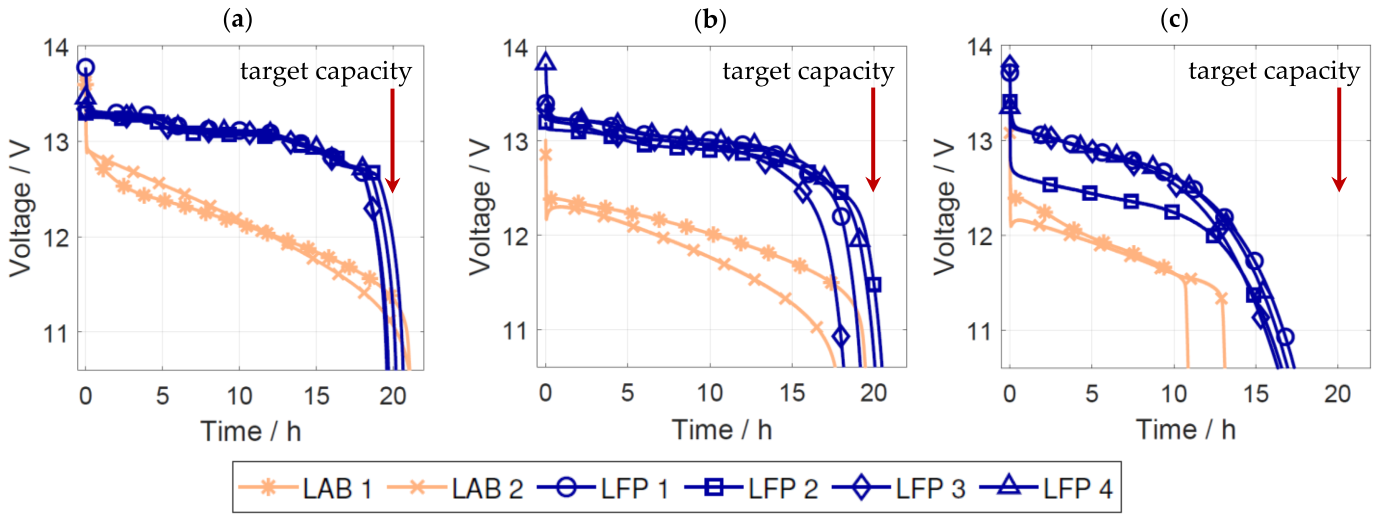

Figure 1. C_{20} capacity at (**a**) 25 °C, (**b**) 0 °C, and (**c**) −18 °C.

Figure 2a evaluates the measured C_{20} capacity normalized to their nominal capacity at different temperatures. At 25 °C, the lead–acid batteries provide 107% of their nominal capacity, while the LFP batteries vary from 98% to 103%. For 0 °C, the measured capacity of all batteries decreases down to a range between 91% and 102% of their measured 25 °C capacity. When further decreasing the temperature to −18 °C, the measured capacity of the LFP batteries decreases between 82% and 91% of their measured 25 °C capacity. For decreasing temperatures, the measured C_{20} capacity declines for both technologies but less for LFP batteries than for LABs.

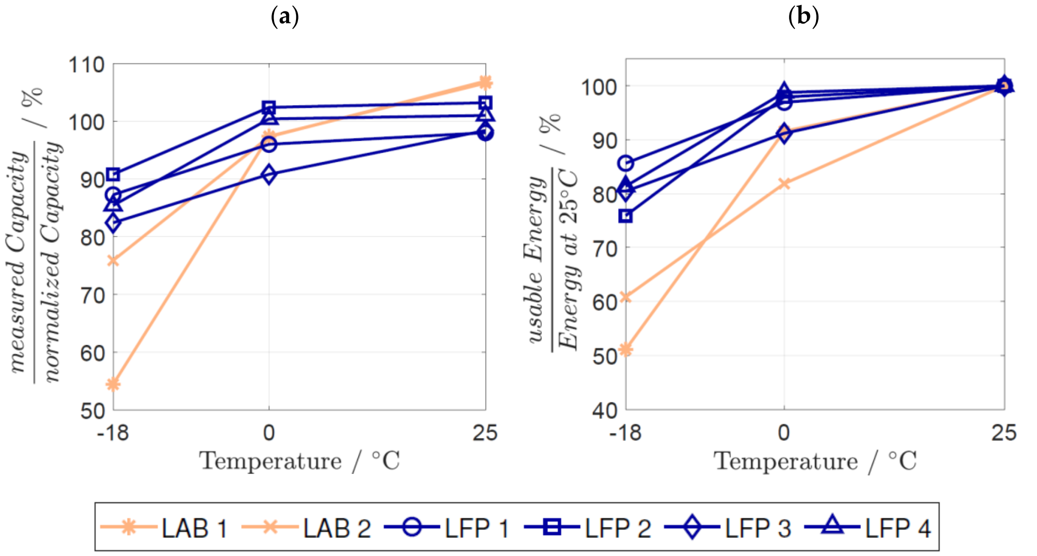

Figure 2. C_{20} capacity test (**a**) measured capacity and (**b**) useable energy.

Figure 2b visualizes the usable energy of each investigated starter battery normalized to its usable energy at 25 °C. At 0 °C, the usable energy for the LABs is between 82% and 91%, and for the LFP batteries, it is between 91% and 99%. At ambient temperatures of −18 °C, the usable energy decreases even further, between 51% and 61% for LABs and between 76% to 86% for LFP batteries. The usable energy declines with lower temperatures for all batteries but less for LFP batteries than for LABs.

3.2. First Pulse of the Cold-Cranking Test

The cold-cranking tests were performed at different temperatures below 0 °C. Figure 3a,b show the cold-cranking voltage of the first 10 s pulse at 0 °C and −10 °C. For these temperatures, all batteries provide the requested discharging current during the first pulse. However, the voltage drop is highly temperature dependent and increases with decreasing temperature for both technologies. Furthermore, the voltage level is higher for the LFP batteries than the LABs, also providing a higher power level.

In Figure 4, the cold-cranking ability is shown for −18 °C, as initially defined by the EN standard [4]. At −18 °C, two out of four LFPs reach their voltage safety limit of 8 V during the first discharging pulse. Even though the shut-off voltage limit of the LFP batteries has already been decreased from the original battery voltage limits of 10.5 V (2.63 V per cell) down to the safety voltage limit found in the cell specification datasheet of 2 V per cell, 8 V for the complete LFP battery. As soon as the voltage limit of 8 V is reached, the discharging current is limited. Therefore, the two LFP batteries cannot provide the requested current demanded by the standard [4].

The LABs do not reach their much lower cut-off voltage limit of 6 V. However, a typical passenger car gasoline engine does not require a certain current but a minimum power for a certain amount of time for the ignition process to function [2]. Additionally, since power is a function of current and voltage, the lower voltage limit for LABs that allows providing the demanded current might still prevent a reliable ignition process. At −18 °C, all batteries provide more than 60 W Ah^{-1} power for the first 10 s pulse. Therefore, independent of the technology, at −18 °C, a 33.3 Ah up to 43.3 Ah battery could provide the required power of 2 kW up to 2.6 kW for the ignition process [2].

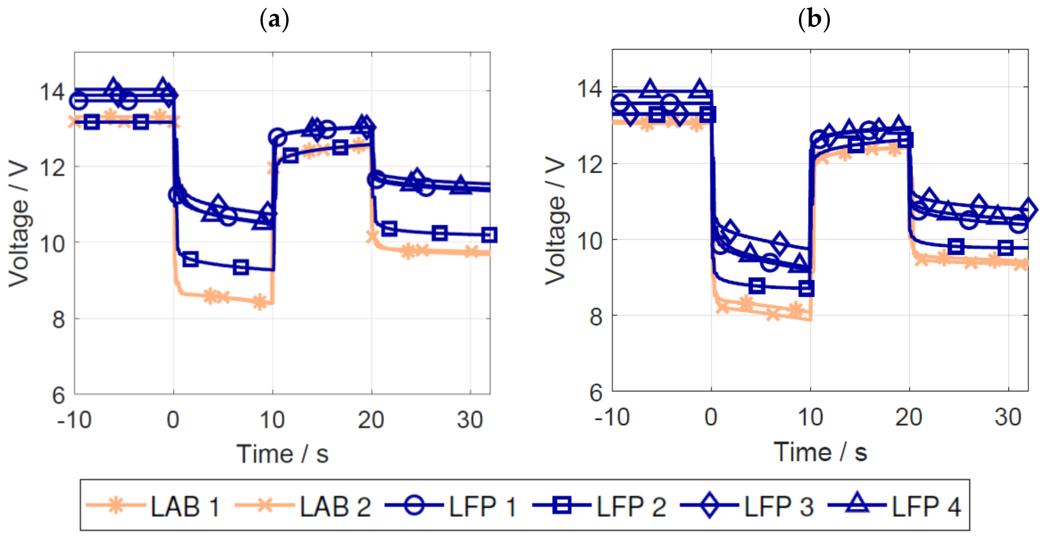

Figure 3. Cold-cranking test (**a**) at 0 °C and (**b**) at −10 °C.

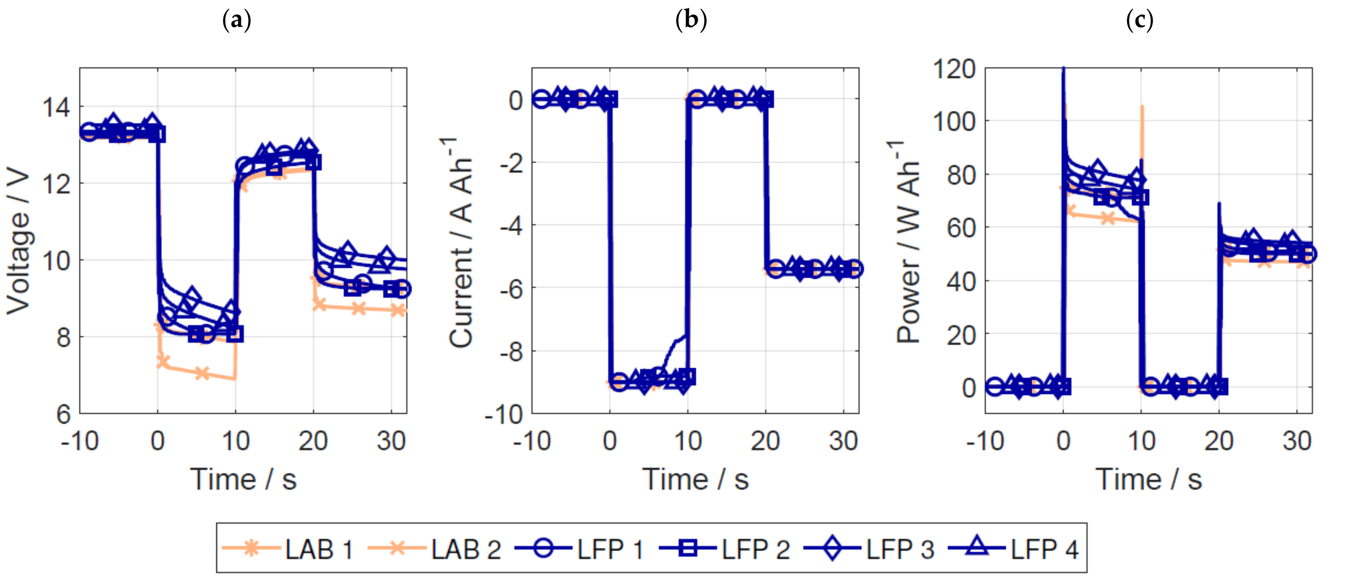

Figure 4. First pulse of the cold-cranking test at −18 °C: (**a**) voltage, (**b**) current, and (**c**) power.

Results of the cold-cranking performance at −30 °C are shown in Figure 5. At −30 °C, all batteries have reached their safety limit during the first discharging pulse. Therefore, neither the LABs nor the LFP batteries can provide the requested current demanded by the standard [4]. Compared to the LFP batteries, the LABs reach the limit much later and even almost pass the criteria. However, the LABs provide between 60 W Ah^{-1} and 50 W Ah^{-1} during the first discharging pulse. The power level of the LFP batteries during the first pulse is even lower.

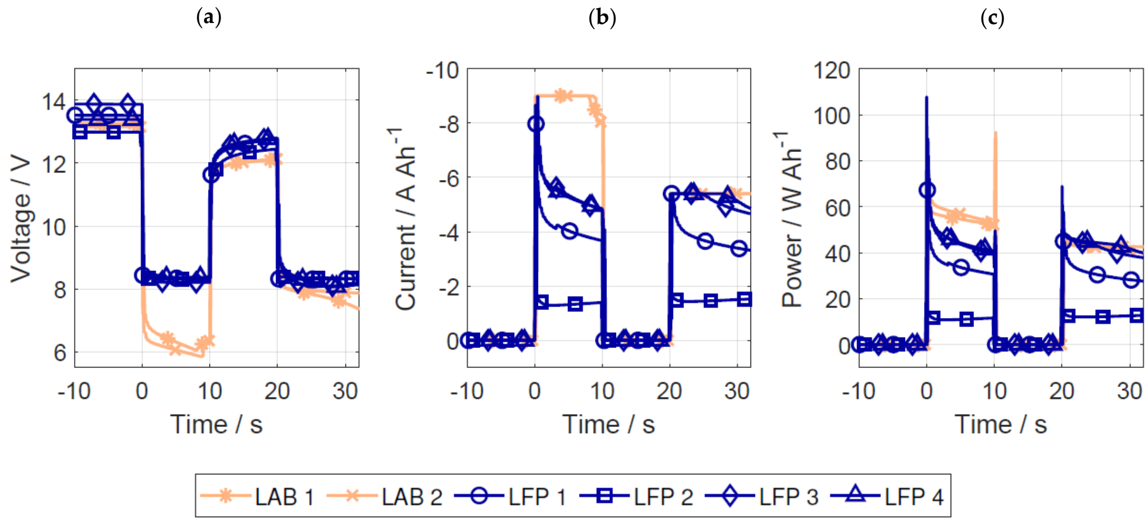

Figure 5. First pulse of the cold-cranking test at −30 °C: (**a**) voltage, (**b**) current, and (**c**) power.

Furthermore, the energy output has been evaluated. A certain power must be delivered for a certain amount of time to start an engine. Therefore, the total and usable energy of the starter batteries is more meaningful for the qualitative comparison between the technologies. The total energy E_{total} can be calculated using the average open circuit voltage V_{av} and the discharging current I during the first 10 s pulse:

$$E_{total} = V_{av} \int_{0\ s}^{10\ s} I(t)\ dt$$

For determining the average open circuit voltage, the voltage level before the first discharging pulse and the relaxation voltage at the end of the 10 s pause are used. The average of both voltages will approximate the open circuit voltage during the first discharging pulse. Since the relaxation processes outlast the 10 s pause, the determined average voltage will be underestimated.

The usable energy E_{use} is determined using the actual voltage and current during the first 10 s discharging pulse:

$$E_{use} = \int_{0\ s}^{10\ s} V(t) \cdot I(t)\ dt$$

Illustrations of the voltages used for the total and usable energy estimation are shown in Figure 6a,b.

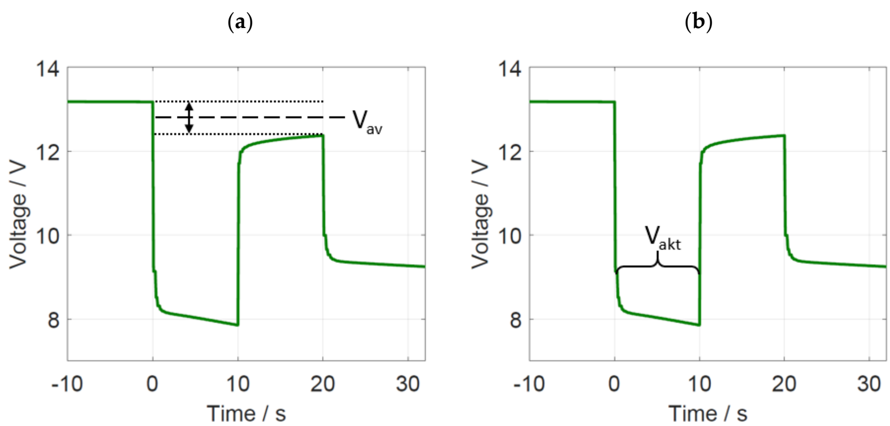

Figure 6. Illustration of the voltages used for determining (**a**) the total energy and (**b**) the usable energy during the first pulse of the cold-cranking test.

The total energy degradation from 0 °C to −30 °C is shown in Figure 7a. For LABs, the total energy decreases by less than 2% between 0 °C and −30 °C, whereas LFP batteries experience a decrease to 6% of the total energy by reducing the temperature from 0 °C to −18 °C. At −30 °C, the total energy of the LFP batteries is only 15% to 60% of the total energy measured at 0 °C. Thus, the investigated LABs provide a higher total energy over the tested temperature range.

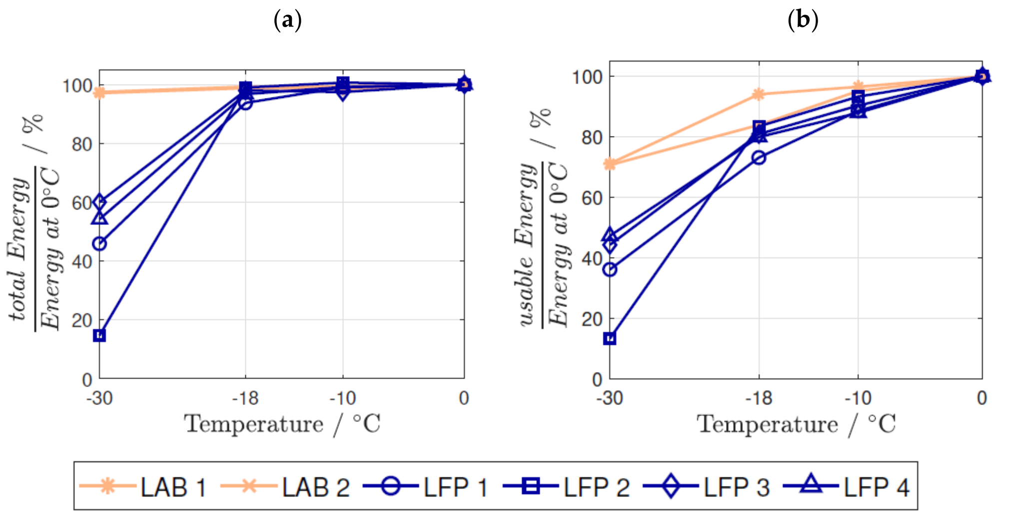

Figure 7. During the first pulse of cold-cranking test (**a**) total energy and (**b**) usable energy.

As visualized in Figure 7b, the usable energy degradation shows a higher decrease for all batteries compared to the total energy. As energy is used for internal heating of the battery, the useable energy is lower. LABs provide higher usable energy values for the investigated temperatures below 0 °C. The LFP batteries have a comparable but slightly less usable energy decrease than LABs at temperatures above and including −18 °C. However, at −30 °C, the usable energy of the LFP batteries decreases drastically.

Combining the total and the usable energy, the efficiency, shown in Figure 8, can be determined with

$$E_{Eff} = \frac{E_{usable}}{E_{total}}$$

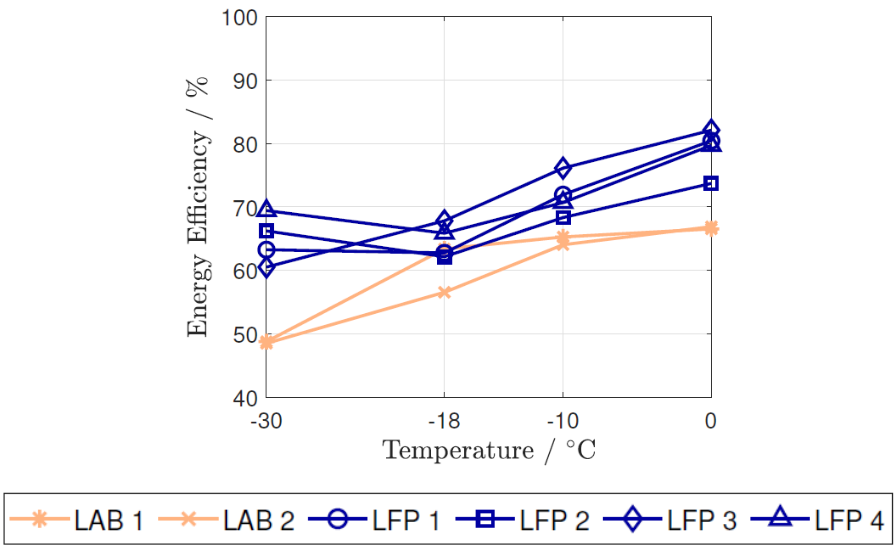

Figure 8. Energy efficiency during first pulse of cold-cranking test.

The energy efficiency during the first pulse of the cold-cranking test is higher for LFP batteries compared to LABs for all investigated ambient temperatures. The efficiency decreases for decreasing temperatures, independent of the technology used. However, the efficiency increases at −30 °C again. This can be explained by the temperature influence on the relaxation voltage after the 10 s pause. The relaxation takes longer at lower temperatures. Therefore, the voltage underestimation is more significant at −30 °C. Therefore, the calculated V_{av} decreases significantly for some batteries at −30 °C. On the basis of this estimation, E_{total} decreases, and the efficiency increases compared to −18 °C.

The internal resistance measured with a Hioki (1 kHz resistance) at different ambient temperatures is shown in Figure 9. The internal resistance of all batteries increases with decreasing temperatures. This is one reason why the cold-cranking performance decreases with decreasing temperatures. However, the internal resistances of the LABs and the LFP batteries are in the same range for all temperatures. Therefore, the internal resistance alone does not explain why the LABs have a much higher power output and reach the voltage limit during the first discharge pulse much later than the LFP batteries. LABs and LFP batteries are very different electrochemical systems with different temperature dependencies of the chemical reaction rate and diffusion speed, also affecting the cold-cranking performance.

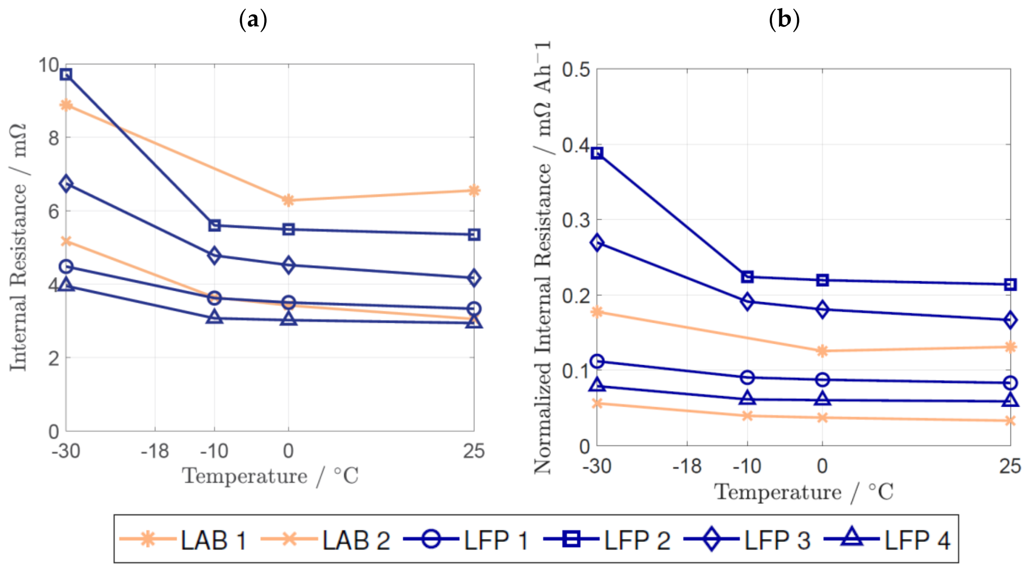

Figure 9. Internal resistance: (**a**) absolute values and (**b**) normalized values.

3.3. Second Pulse of the Cold-Cranking Test

Even though the starting voltage level decreases with decreasing temperature, all LFP batteries were able to provide the required current during the second pulse of the cold-cranking test at 0 °C, −10 °C, and −18 °C, shown in Figures A1–A3. For all LFP batteries, the voltage rises significantly during the second discharging pulse. Most likely caused by self-heating. After 200 s of the cold-cranking test, the voltage level of all LFP batteries is at a similar level, independent of the ambient temperature.

The cold-cranking results of the LABs at 0 °C, −10 °C, and −18 °C, shown in Figures A1–A3, show a lower voltage curve than the LFP batteries. Contrary to the LFP batteries, the voltage level of the LABs does not increase during the second pulse of the cold-cranking test. The heat capacity of the LABs is much higher than that of the LFP batteries. Therefore, temperature changes would take longer and cannot affect the results of a 200 s test duration. LAB 1 has a much shorter discharging time than LAB 2, independent of the ambient temperature. LAB 2 provides the required current at 0 °C, −10 °C, and −18 °C.

At −30 °C, shown in Figure 10, all LFP batteries reach the 8 V limit right at the beginning of the second pulse. After some seconds, the voltage increases again, and the requested current can be delivered at the end of the second pulse. The LABs, on the other hand, can provide the requested current but suffer a significant voltage decrease during the first seconds of the second pulse. This results in a marginally smaller power during the first seconds of the second discharging pulse of the LABs at −30 °C compared to −18 °C and compared to the LFP batteries at −30 °C as well.

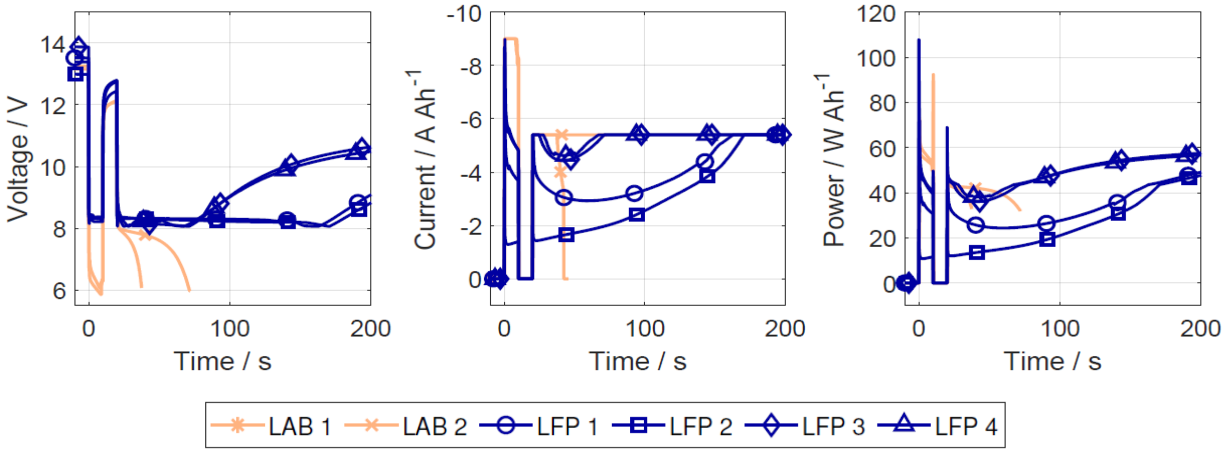

Figure 10. Complete cold-cranking test at −30 °C: (**a**) voltage, (**b**) current, and (**c**) power.

Table 5 summarizes the average power of all batteries during the first and the second pulse at the investigated temperatures. Moreover, Table 5 evaluates if the battery passed the test defined by the standard at a given temperature.

Table 5. Passing of the standard and average power during 1st and the 2nd pulse.

ID	Ambient Temperature	Passing the Standard	Average Power 1st Pulse	Average Power between 20 s and 60 s
LAB1	0 °C	passed	77.4 W Ah^{-1}	51.7 W Ah^{-1}
	−10 °C	passed	74.8 W Ah^{-1}	50.3 W Ah^{-1}
	−18 °C	passed	72.8 W Ah^{-1}	49.4 W Ah^{-1}
	−30 °C	not passed	55.1 W Ah^{-1}	20.6 W Ah^{-1}
LAB2	0 °C	passed	77.3 W Ah^{-1}	52.3 W Ah^{-1}
	−10 °C	passed	73.6 W Ah^{-1}	50.2 W Ah^{-1}
	−18 °C	passed	64.8 W Ah^{-1}	46.6 W Ah^{-1}
	−30 °C	not passed	54.6 W Ah^{-1}	41.7 W Ah^{-1}
LFP1	0 °C	passed	96.8 W Ah^{-1}	61.1 W Ah^{-1}
	−10 °C	passed	85.8 W Ah^{-1}	55.8 W Ah^{-1}
	−18 °C	not passed	70.8 W Ah^{-1}	49.7 W Ah^{-1}
	−30 °C	not passed	35.0 W Ah^{-1}	27.1 W Ah^{-1}
LFP2	0 °C	passed	85.3 W Ah^{-1}	55.2 W Ah^{-1}
	−10 °C	passed	79.6 W Ah^{-1}	52.9 W Ah^{-1}
	−18 °C	not passed	71.2 W Ah^{-1}	50.5 W Ah^{-1}
	−30 °C	not passed	11.3 W Ah^{-1}	13.5 W Ah^{-1}
LFP3	0 °C	passed	99.4 W Ah^{-1}	62.2 W Ah^{-1}
	−10 °C	passed	89.8 W Ah^{-1}	58.1 W Ah^{-1}
	−18 °C	passed	80.4 W Ah^{-1}	54.0 W Ah^{-1}
	−30 °C	not passed	44.0 W Ah^{-1}	38.2 W Ah^{-1}

Table 5. *Cont.*

ID	Ambient Temperature	Passing the Standard	Average Power 1st Pulse	Average Power between 20 s and 60 s
LFP4	0 °C	passed	97.1 W Ah^{-1}	61.5 W Ah^{-1}
	−10 °C	passed	85.6 W Ah^{-1}	56.8 W Ah^{-1}
	−18 °C	passed	77.6 W Ah^{-1}	52.7 W Ah^{-1}
	−30 °C	not passed	45.8 W Ah^{-1}	40.4 W Ah^{-1}

4. Conclusions

Six test cells, two LABs, and four LFP batteries from different manufacturers have been tested regarding their low-temperature capability. The capacity was tested at various temperatures between 25 °C and −18 °C using small discharging currents. Thereby, the temperature gradient and changes within the batteries, induced by self-heating during the discharge, could be minimized. LFP batteries have higher voltage levels than LABs, which results in a higher power and energy output. Moreover, LFP batteries have a lower capacity decline (82–91% C/C_n at −18 °C) and a lower energy decline (76–86% E/E_n at −18 °C) for decreasing temperature compared to LABs (55–76% C/C_n, 51–61% E/E_n at −18 °C). For low discharging currents, within a temperature range between 25 °C and −18 °C, the LFP batteries are superior.

The cold-cranking ability was tested according to the EN standard. Additionally, to the standard, where the test is only defined for −18 °C, within this work, a temperature range between 0 °C and −30 °C was evaluated. Regarding the standard test definition, the LABs passed the requirements for the first pulse at 0 °C, −10 °C and −18 °C by providing the required current of 9 A Ah^{-1} for 10 s while keeping a voltage above 6 V. The LABs also passed the test requirements during the second pulse of the cold-cranking test, with rapidly decreasing voltage. The LABs almost passed the requirements for the first pulse at −30 °C since the voltage limit was reached and the current had to be decreased, still providing more than 8 A Ah^{-1}. However, the voltage decrease in the LABs during the second pulse at −30 °C is major.

The LFP batteries passed the requirements regarding the test definition for the first and second pulse at 0 °C and −10 °C. At −18 °C only two of the four LFP batteries could provide the required current without falling below the LFP's specific cut-off voltage of 8 V. However, considering the power instead of current, all LFP batteries could deliver a similar power as the lead–acid batteries at −18 °C during the first pulse and all passed the requirements of the second pulse at −18 °C. At all temperatures, the voltage level increased during the second pulse of the cold-cranking test. This is caused by the self-heating of the LFP batteries, which have a relatively low heat capacity compared to the LABs. All LFP batteries failed the test requirements for the first and second pulse at −30 °C. However, through self-heating, the LFP can provide the required current at the end of the second cold-cranking pulse.

The minimum voltage is the decision criterion for passing the EN cold-cranking standard test. Even if the nominal voltage is similar between the LAB and the LFP battery, the cut-off voltage differs from 6 V for LABs to 8 V for LFP batteries. Thereby, the test is not comparable for different technologies. For comparability between technologies, the requirements of the standard test should be redefined in terms of power or energy. In terms of energy and power, the LFP battery can generate comparable cold-cranking results till −18 °C. The LABs are superior during cold-cranking tests at temperatures below −18 °C.

Author Contributions: Conceptualization, F.W.; methodology, S.B. and J.K.; software, S.B.; validation, S.B. and A.S.; formal analysis, S.B.; investigation, S.B. and A.S.; data curation, S.B.; writing—original draft preparation, S.B. and F.W.; writing—review and editing, S.B., J.K., F.W. and A.S.; visualization, S.B.; supervision, J.K.; project administration, S.B.; funding acquisition, F.W. and J.K. All authors have read and agreed to the published version of the manuscript.

Funding: This research was funded by IBB Business Team GmbH. We acknowledge support by the German Research Foundation and the Open Access Publication Fund of TU Berlin.

Institutional Review Board Statement: Not applicable.

Informed Consent Statement: Not applicable.

Data Availability Statement: Data available on request.

Acknowledgments: The authors would like to thank the battery manufacturers that have provided their batteries for this project and TGM Lightweight Solutions GmbH for the support and many discussions.

Conflicts of Interest: The authors declare no conflict of interest. The funders had no role in the design of the study; in the collection, analyses, or interpretation of data; in the writing of the manuscript; or in the decision to publish the results.

Appendix A

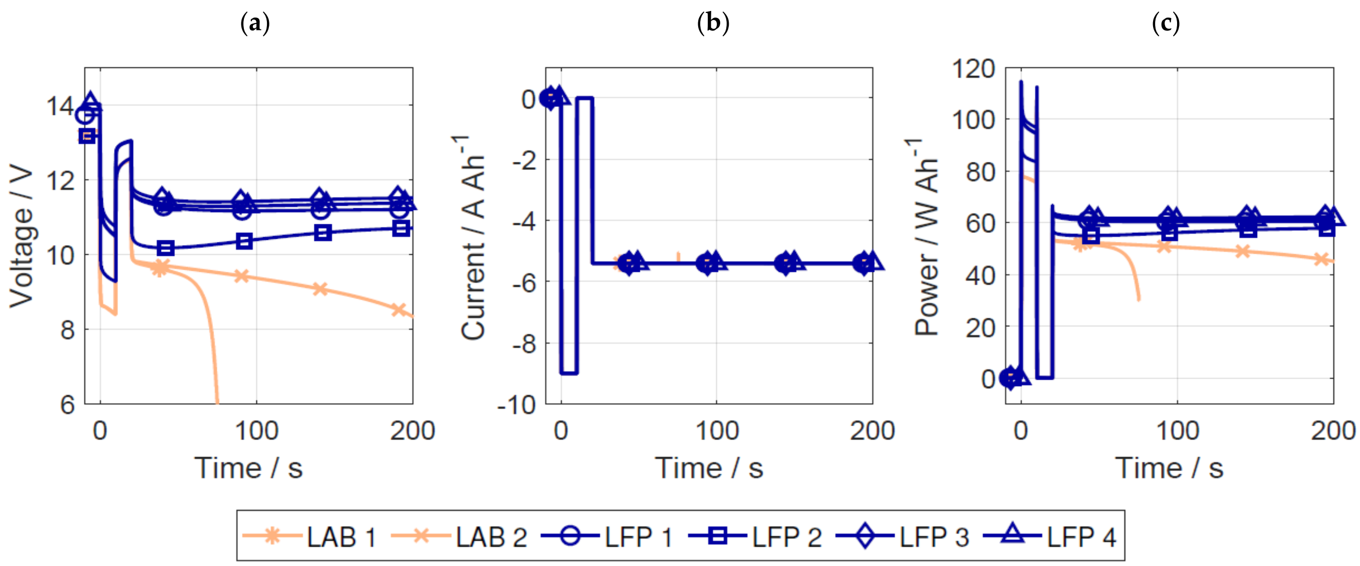

Figure A1. Complete cold-cranking test at 0 °C: (**a**) voltage, (**b**) current, and (**c**) power.

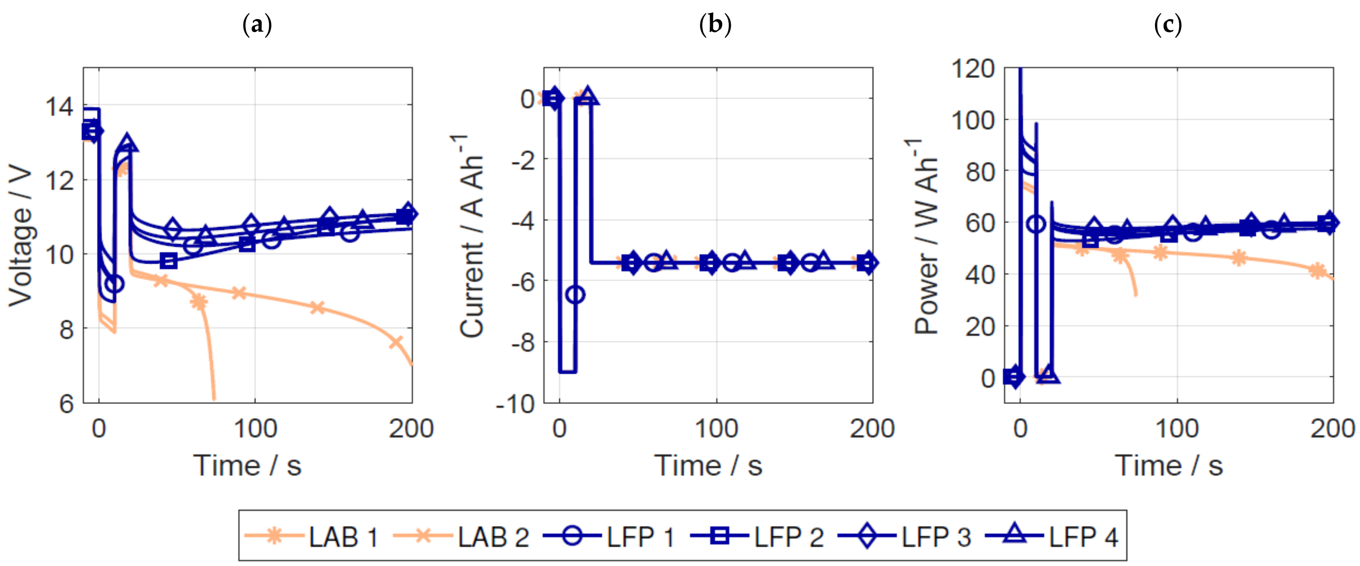

Figure A2. Complete cold-cranking test at −10 °C: (**a**) voltage, (**b**) current, and (**c**) power.

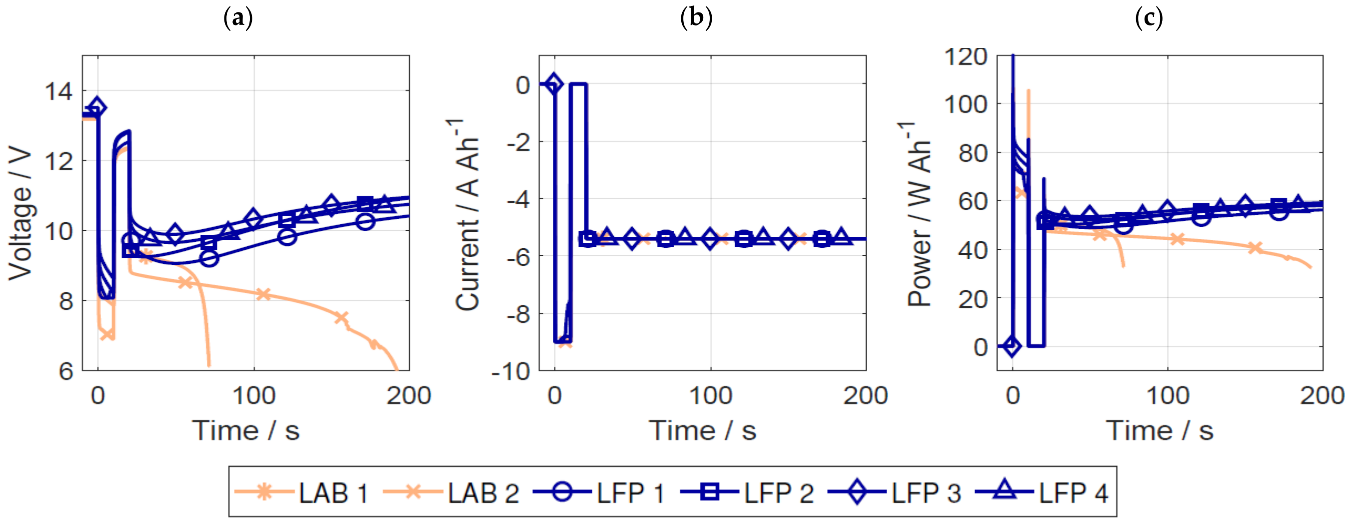

Figure A3. Complete cold-cranking test at −18 °C: (**a**) voltage, (**b**) current, and (**c**) power.

References

1. Borgeest, K. *Elektronik in der Fahrzeugtechnik*; Springer Fachmedien: Wiesbaden, Germany, 2010; ISBN 978-3-8348-0548-5.
2. Reif, K. *Batterien, Bordnetze und Vernetzung*; Vieweg+Teubner Verlag/GWV Fachverlage GmbH Wiesbaden: Wiesbaden, Germany, 2010; ISBN 978-3-8348-1310-7.
3. Vergossen, D. *Differenzierte Betrachtung und Bewertung von 12-Volt-Lithium-Ionen-Starterbatterien in PKW-Bordnetzen*; Dissertation; Eric Cuvillier: Göttingen, Germany, 2018.
4. *Lead-Acid Starter Batteries, Part I: General Requirements and Methods of Test*; European Committee for Electrotechnical Standardisation: Brussels, Belgium, 2019.
5. Pischinger, S.; Seiffert, U. *Vieweg Handbuch Kraftfahrzeugtechnik*; Aktualisierte und erweiterte Auflage; Springer Vieweg: Wiesbaden, Germany, 2016; ISBN 978-3-658-09528-4.
6. Reif, K. *Kraftfahrzeug-Hybridantriebe: Grundlagen, Komponenten, Systeme, Anwendungen*; Vieweg+Teubner Verlag Imprint: Wiesbaden, Germany, 2012; ISBN 978-3-8348-2050-1.
7. Porsche. New Lightweight Battery Option for the Porsche 911 GT3, 911 GT3 RS, and Boxster Spyder: World Debut: Starter Battery in Lithium-Ion Technology. Available online: https://www.porsche.com/usa/aboutporsche/pressreleases/pag/?pool=international-de&id=2009-11-23-02 (accessed on 9 December 2019).
8. Ferg, E.E.; Schuldt, F.; Schmidt, J. The challenges of a Li-ion starter lighting and ignition battery: A review from cradle to grave. *J. Power Sour.* **2019**, *423*, 380–403. [CrossRef]
9. Fehrenbacher, C. 12V Li-Ion Batteries—Ready for Mainstream Adoption. In Proceedings of the Advanced Automotive Battery Conference, Detroit, MI, USA, 14–17 June 2016.
10. Yang, X.-G.; Liu, T.; Wang, C.-Y. Thermally modulated lithium iron phosphate batteries for mass-market electric vehicles. *Nat. Energy* **2021**, *6*, 176–185. [CrossRef]
11. Doughty, D.; Roth, E.P. A General Discussion of Li Ion Battery Safety. *Electrochem. Soc. Interface* **2012**, *21*, 37–44. [CrossRef]
12. Smart, M.C.; Ratnakumar, B.V.; Surampudi, S. Use of Organic Esters as Cosolvents in Electrolytes for Lithium-Ion Batteries with Improved Low Temperature Performance. *J. Electrochem. Soc.* **2002**, *149*, A361–A370. [CrossRef]
13. Smart, M.C.; Ratnakumar, B.V.; Surampudi, S. Electrolytes for Low-Temperature Lithium Batteries Based on Ternary Mixtures of Aliphatic Carbonates. *J. Electrochem. Soc.* **1999**, *146*, 2. [CrossRef]
14. *Battery Test Manual For 12 Volt Start/Stop Vehicles*, 1st ed.; INL/EXT-12-26503; Idaho National Labaratory: Idaho Falls, ID, USA, 2015.
15. Jaguemont, J.; Boulon, L.; Dubé, Y. A comprehensive review of lithium-ion batteries used in hybrid and electric vehicles at cold temperatures. *Appl. Energy* **2016**, *164*, 99–114. [CrossRef]